TWENTYFIFTH EUROPEAN ROTOCRAFT FORUM

Paper No. G1

MODAL ANALYSIS OF AEROELASTIC RESPONSE OF A HOVERING ROTOR – THE IMPACT OF THE MODE CHOICE

BY

M. GENNARETTI
University Roma Tre, Italy

A. CORBELLI, F. MASTRODDI, L. BALIS CREMA
University of Rome 'La Sapienza', Italy

SEPTEMBER 14–16, 1999
ROME
ITALY

ASSOCIAZIONE INDUSTRIE PER L'AEROSPAZIO, I SISTEMI E LA DIFESA
ASSOCIAZIONE ITALIANA DI AERONAUTICA E ASTRONAUTICA

MODAL ANALYSIS OF AEROELASTIC RESPONSE OF A HOVERING ROTOR – THE IMPACT OF THE MODE CHOICE

M. GENNARETTI
University Roma Tre
Dipartimento di Ingegneria Meccanica e Industriale, Rome, Italy

A. CORBELLI, F. MASTRODDI, L. BALIS CREMA
University of Rome 'La Sapienza'
Dipartimento Aerospaziale, Rome, Italy

ABSTRACT

The aim of this paper is the aeroelastic analysis of the elastic motion of a cantilever blade in flap-lag-torsion motion. Specifically, we investigate on the convergence behavior of the solutions obtained using different approaches for the elastic displacement description. Three different mode shape sets are used in Galerkin's method approaches, and their solutions are also compared with those obtained from a FEM approach. The aerodynamic model used in this work is the simple very-low frequency approximation of the pulsating-free-stream Greenberg extension of the Theodorsen theory. Numerical investigation is performed both for determining the aeroelastic stability boundaries of the blade and for analyzing the frequency response to a vertical pulsating free-stream velocity.

1. INTRODUCTION

The subject of this work is the aeroelastic stability and response analyses of hingeless cantilever rotor blades, with emphasis on the solution accuracy and convergence behavior, as a function of the approach used for the elastic-motion description.

In the aeroelastic analysis of helicopter rotors, the structural dynamics of the blades is often formulated in terms of a series of mode shapes whose coefficients (mode amplitudes) may be interpreted as the time-dependent Lagrangean variables (generalized coordinate) of the structure. This approach assures convergence of the solution in terms of stability analysis, faster than alternate descriptions of the elastic displacement (*e.g.*, finite elements, consisting of using non-orthogonal piecewise-defined shape functions). From a practical point of view, it means that if a certain level of accuracy of the stability analysis is obtained by using M linearly independent modes (and corresponding Lagrangean variables), the same level of accuracy may be reached by using a larger number $N > M$ of non-orthogonal shape functions (and corresponding Lagrangean variables). Nonetheless, it is possible to observe a different convergence behavior of the solution, if this is analyzed in terms of local stress levels. For instance, for a cantilever blade, if one considers the root elastic bending moment as the parameter to be studied in the aeroelastic analysis, then the convergence of the modal approach solution could be found to be slower than that obtained from a FEM approach (that uses locally defined shape functions). Therefore, the best choice for the description of the elastic displacement depends generally on the target of the performed aeroelastic analysis.

Several types of mode shapes may be used in rotor blade structural dynamic analysis. Among them, there are the set of eigenfunctions of the blade structural operator defined in the rotating frame (rotating free-vibration modes), and the set of eigenfunctions of the blade structural operator defined in the non-rotating frame (non-rotating free-vibration modes): the first set of eigenfunctions is influenced by the presence, in the structural operator, of the centrifugal and Coriolis inertial terms, whereas the second set of eigenfunctions does not consider the presence of these inertial terms, which are to be included in the analysis as forcing terms. However, the orthogonal shape functions to be used in the analysis, might also be unrelated to the blade structural operator: for instance, the uncoupled bending and torsion free-vibration modes of a non-rotating uniform beam, have been applied in Refs. [1] and [2] for aeroelastic analysis, whereas the modified Duncan polynomials have been used in Ref. [3]. Furthermore, some authors have also performed aeroelastic analysis of rotor blades applying FEM approaches, and among them Friedmann and Straub [4] developed a FEM formulation for the flap-lag aeroelastic analysis of hovering rotors, whereas Sivaneri and Chopra [5] examined the aeroelastic stability of flap bending, lead-lag bending and torsion of a helicopter rotor in hover using a finite element formulation based on Hamilton's principle.

The aim of this work is a comparison among helicopter-rotor aeroelastic solutions given by different mode-shape decompositions and the application of a finite element approach. Specifically, we wish to investigate about the advantages and disadvantages in using the mode shape approach, with respect to the finite element approach. The comparison will be presented in terms of aeroelastic stability analysis and stress levels prediction on the blade (particularly, at the root of a cantilever hingeless rotors). In performing the aeroelastic analysis, the unsteady aerodynamic loadings will be described by the simple quasi-steady approximation of the Greenberg formulation obtained extending the Theodorsen theory to pulsating free-stream velocity [6].

2. BLADE STRUCTURAL AND AERODYNAMIC MODELS

In order to achieve the purposes of the present work, we have chosen to use classical and quite simple models both for structural dynamics and for aerodynamic loadings acting on the blade.

The rotor blade considered here is a hingeless blade structurally modeled as a cantilever slender beam, undergoing flap bending, chordwise bending and torsion. A realistic hingeless rotor configuration is defined by lots of parameters that influence both the steady state blade stress distribution and the blade stability characteristics. Such parameters are precone, droop, torque offset and sweep that in this work, except for the precone angle, have been considered to be equal to zero. An additional fundamental element in a hingeless rotor description is the flexibility of the pitch link devoted to the actuation of blade motion controlled by the swash plate: it is a major factor in the structural coupling between flap bending, lead-lag bending and torsion, and hence influences the aeroelastic behavior of the blade. Furthermore, coupling between bending and torsion elastic deflections is strongly influenced also by parameters like the positions of the mass center, tension center, elastic center and the aerodynamic center. All these depend on the blade construction features and shape and have a great impact on its stability characteristics. For the sake of simplicity, in this work we have assumed no chordwise offsets of the elastic axis, tension axis and center-of-mass axis.

Under all the simplifying assumptions mentioned above and considering untwisted blades with uniform mass and stiffness spanwise distribution, the equations of motion governing the blade structural dynamics are those given in Ref. [1], that are the corresponding simplified version of those derived in Ref. [7]. These equations are a set of coupled integro-partial differential equations with unknowns the lateral in-plane displacement of the elastic axis, $v(x,t)$, the lateral out-of-plane displacement of the elastic axis, $w(x,t)$, and the cross-section elastic torsion deflection $\varphi(x,t)$. Their expressions are

of the following type (see Ref. [1] for details):

$$m\,\ddot{v} + \mathcal{O}_v[v, w, \varphi, \dot{v}, \dot{w}] = \mathcal{L}_v \tag{1}$$

$$m\,\ddot{w} + \mathcal{O}_w[v, w, \varphi, \dot{v}, \dot{w}] = \mathcal{L}_w \tag{2}$$

$$J_\varphi\,\ddot{\varphi} + \mathcal{O}_\varphi[v, w, \varphi] = \mathcal{M}_\varphi, \tag{3}$$

where m denotes the blade mass per unit length, J_φ denotes the cross-section torsional mass moment of inertia, $\mathcal{O}_v$ and $\mathcal{O}_w$ denote fourth-order in space, nonlinear, integro-partial differential operators, whereas $\mathcal{O}_\varphi$ denotes a second-order in space, nonlinear, partial differential operator. Furthermore, $\mathcal{L}_v$ and $\mathcal{L}_w$ are, respectively, the in-plane and out-of-plane aerodynamic forces per unit length acting on the blade, whereas $\mathcal{M}_\varphi$ is the aerodynamic pitching moment per unit length acting on the blade.

Observing equations (1)–(3) it is apparent that a very important role in rotor blade aeroelastic predictions is played by the aerodynamic model applied in describing the forcing terms $\mathcal{L}_v, \mathcal{L}_w, \mathcal{M}_\varphi$. This is true for fixed-wing aeroelastic applications, but its importance is further amplified in rotary-wing aeroelastic analysis due to the complexity of the unsteady aerodynamic field generated by the rotor blades. In particular, the shape of the vortical wake generated by the blades is such that the velocity that it induces on the rotor has a great impact on the unsteady aerodynamic loading distributions, and the accurate description of this velocity field is a fundamental requirement for a realistic aerodynamic field prediction. Furthermore, in rotor aerodynamics the effects due to the 3-D flow are much stronger than in the case of fixed-wing aerodynamics, and this is an additional element of complexity that generally makes unsatisfactory the application of two-dimensional analytical aerodynamic models. Nonetheless, in this work we have applied a very simple quasi-steady, two-dimensional aerodynamic model. This choice has been suggested by the desire of having a simple explicit expression of the aerodynamic loadings in terms of the structural dynamics unknowns of the problem, so as to concentrate the analysis on the role played on the solution accuracy and rate of convergence, by the type of spatial description used for the elastic displacement approximate expressions. Following the approach used in Ref. [1], $\mathcal{L}_v, \mathcal{L}_w, \mathcal{M}_\varphi$ have been obtained from the very-low frequency approximation of the pulsating-free-stream Greenberg extension of the Theodorsen theory for the prediction of unsteady lift and pitching moment on airfoil in unsteady motion [6], with the inclusion of the effects of the wake-induced velocity on the aerodynamic force direction. The resulting formulae for $\mathcal{L}_v, \mathcal{L}_w, \mathcal{M}_\varphi$ are explicit functions of $\varphi, v', w', w'', \dot{v}, \dot{w}, \dot{\varphi}$, and $\ddot{w}$, that combined with equations (1)–(3) yield the final closed-loop flap-lag-torsion aeroelastic equations of motion analyzed in this work.

3. MODAL-APPROACH SOLUTION

As mentioned in Section 1, the aeroelastic equations of motion described above have been solved following both a modal approach and a FEM approach, in order to compare their solutions accuracy, their rate of convergence, and then analyse advantages and disadvantages of the two. In this section we outline the solution scheme obtained by applying the modal approach.

The set of coupled integro-partial differential equations (1)–(3) has been transformed into a set of ordinary differential equations in time, by Galerkin's method. First, the elastic deflections have been expressed in terms of the following series

$$v(x,t) = \sum_{n=1}^{N} q_n^v(t)\,\Phi_n^v(x) \tag{4}$$

$$w(x,t) = \sum_{n=1}^{N} q_n^w(t)\,\Phi_n^w(x) \tag{5}$$

$$\varphi(x,t) = \sum_{n=1}^{N} q_n^{\varphi}(t)\, \Phi_n^{\varphi}(x), \tag{6}$$

where $q_n^v, q_n^w, q_n^\varphi$ denote the generalized coordinates of the problem, whereas $\Phi_n^v, \Phi_n^w, \Phi_n^\varphi$ are sets of linearly independent shape functions (mode shapes), whose choice influences accuracy and rate of convergence of the solution. Next, substituting equations (4)-(6) into equations (1)–(3), the Galerkin method yields a set of $3N$ nonlinear, ordinary differential equations in terms of the generalized coordinates of the problem. Then, the aeroelastic solution is determined from their linearized version for small perturbation motions about the equilibrium configuration. Specifically, expressing the generalized coordinates in terms of the steady equilibrium value and of a small perturbation quantity (*i.e.*, assuming, for instance, $q_n^v(t) = q_{0n}^v + \Delta q_n^v(t)$), a nonlinear algebraic problem with unknowns $q_{0n}^v, q_{0n}^w, q_{0n}^\varphi$ is first formulated and solved by the Newton-Raphson method, and then $3N$ linear differential equations for the small perturbation motion are determined, with coefficients depending on the equilibrium solution. The $3N$ small perturbation equations have the following form

$$\mathsf{M}\,\ddot{\mathsf{q}} + \mathsf{C}\,\dot{\mathsf{q}} + \mathsf{K}\,\mathsf{q} = 0, \tag{7}$$

where $\mathsf{q}^T = \{\Delta q_n^v, \Delta q_n^w, \Delta q_n^\varphi\}$ is the row matrix containing the small perturbation motion unknowns, M is a symmetric matrix containing structural and aerodynamic mass terms, C is an asymmetric matrix containing gyroscopic and aerodynamic damping terms, whereas K is an asymmetric matrix containing structural and aerodynamic stiffness terms.

In this work, three different sets of mode shapes have been employed: *i)* the first set is that given by the eigenfunctions of the cantilever, uniform beam, for which $\Phi_n^v \equiv \Phi_n^w$; *ii)* the second set of mode shapes used in equations (4)-(6), are the eigenfunctions of the rotating uniform beam (incidentally, in the case of the rotor blade considered in this work and for collective pitch angle set equal to zero, is governed by the (decoupled) integro-partial differential equations given by Houbolt and Brooks in Ref. [8]); *iii)* the last set of mode shapes used is that given by the eigenfunctions of the small perturbation equations (7) in vacuo and without gyroscopic terms (*i.e.*, those obtained neglecting both aerodynamic terms and Coriolis force contribution), and therefore is dependent on the steady equilibrium condition examined in the stability or response analysis. The analysis of the behavior of the solutions corresponding to these mode-shape sets is one of the goals of the present paper, and is performed in order to give an idea about how convenient is the use of simple mode shapes in the modal solution approach.

4. FEM-APPROACH SOLUTION

In this section we briefly outline the finite-element formulation used in this work for the aeroelastic analysis of the hingeless rotor blade described above.

For the sake of simplicity, in this phase of the work the finite element formulation has been applied to the elastic blade equations of motion presented in Ref. [8], which are applicable only to the quite narrow range of blade dynamic configurations consisting of both small steady equilibrium deflections, and small unsteady perturbation deflections. Therefore, following the expression of the Hamilton principle given in Ref. [8] (which the reader can also refere to for all the notations and symbols used in the following), and indicating with $\mathcal{U}$ the total strain energy and with $\mathcal{V}$ the work performed by the centrifugal body forces and the applied loading, we have

$$\mathcal{U} - \mathcal{V} = \frac{1}{2}\int_0^R \mathcal{F}(v, w, \varphi, v', w', \varphi', v'', w'', p_y, p_z, q)\, \mathrm{d}x \tag{8}$$

where $\mathcal{F}$ denotes the energetic functional whose expression is given Ref. [8], p_y, p_z, and q represent the applied loading given by the sum of the aerodynamic loadings, $\mathcal{L}_v$, $\mathcal{L}_w$, and $\mathcal{M}_\varphi$, and of the inertial loadings.

Next, we describe the finite element formulation that has been applied to equation (8). Let us divide the blade into a finite number, N_e, of beam elements located on the elastic axis, ξ, coinciding with the radial axis x starting from the shaft (η will denote the chordwise axis, and ζ the axis orthogonal to ξ and η). Therefore, $N_e + 1$ nodes are also defined and six degrees of freedom may be associated to each node: following the standard FE procedure, these are the three translations denoted with u^e, v^e, and w^e (in ξ, η, and ζ direction respectively), and the three rotations φ, r_w, and r_v around the ξ, η, and ζ axis, respectively.

Considering the generic beam finite element with nodes denoted by a and b, in the finite element formulation the displacement vector $\mathbf{u}^e$ (with components u, v, and w) is approximated as

$$\begin{aligned} \mathbf{u}^e(\xi,\eta,\zeta,t) &= u_a^e\Phi_1^e + v_a^e\Phi_2^e + w_a^e\Phi_3^e + \phi_a^e\Phi_4^e + r_{w_a}^e\Phi_5^e + r_{v_a}^e\Phi_6^e \\ &+ u_b^e\Phi_7^e + v_b^e\Phi_8^e + w_b^e\Phi_9^e + \phi_b^e\Phi_{10}^e + r_{w_b}^e\Phi_{11}^e + r_{v_b}^e\Phi_{12}^e, \end{aligned} \tag{9}$$

where the subscripts a and b indicate that the d.o.f.'s are referred to the node a and b, respectively, whereas vectors $\mathbf{\Phi}_i^e$ are the the standard finite element shape functions for a beam element. From equation (9), in terms of components, the elastic displacement vector may be expressed as

$$\mathsf{u}^e(\xi,\eta,\zeta,t) = \mathsf{A}^e(\xi,\eta,\zeta)\,\mathsf{x}^e(t) \tag{10}$$

where u^e is the column matrix containing the components of the vector $\mathbf{u}^e$, x^e is the column matrix containing the twelve element d.o.f.'s, and the matrix A^e contains the finite element shape functions, as described, for instance, in Ref. [9].

Next, considering all the finite elements of discretization of the blade and substituting for each of them equation (10) into equation (8), one obtains the discrete form of the energetic functional of the aeroelastic problem. Thus, requiring to the energy defined by equation (8) to be stationary with respect to the finite element d.o.f.'s, one obtains the following final finite element dynamic equation for the generic element

$$\mathsf{K}^e\mathsf{x}^e + \mathsf{K}_C^e\mathsf{x}^e = \mathsf{e}^e \tag{11}$$

where e^e is the column matrix containing the external loadings (aerodynamic forces and relative inertial forces), K^e is the (standard) stiffness matrix due to the elastic energy, $\mathcal{U}$, whereas K_C is the (equivalent) stiffness matrix taking into account the effects due to due centrifugal loadings, and obtained from the work $\mathcal{V}$.

Finally, following the standard FE procedure, the element consistent $[12 \times 12]$ mass matrix can be defined as:

$$M_{ij}^e = \int_{V^e} \rho\,\mathbf{\Phi}_i^e \cdot \mathbf{\Phi}_j^e\,\mathrm{d}V \tag{12}$$

where ρ denotes the structural density.

Once the stiffness and mass matrices are evaluated for each blade element, the global matrices can be assembled considering the elementary beam topology, and then, observing that $\mathsf{e}^e = -\mathsf{M}^e\ddot{\mathsf{x}} + \mathsf{f}^e$, with f^e denoting the aerodynamic loads, the final equations for the blade dynamics have the form

$$\mathsf{M}\ddot{\mathsf{x}} + (\mathsf{K} + \mathsf{K}_C)\,\mathsf{x} = \mathsf{f}. \tag{13}$$

with trivial meaning for the global matrix M, K, K_C, and C. As already outlined in Section 3, the aerodynamic loads, f, have been dermined from the quasi-steady approximation of the pulsating-free-stream Greenberg extension of the Theodorsen theory.

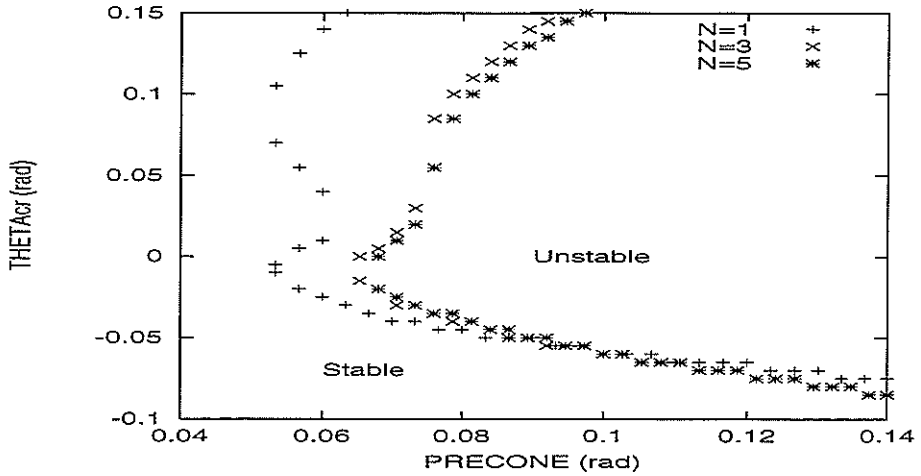

Figure 1: Stability Boundary due to precone angle for soft in-plane blade. Uniform-beam modes.

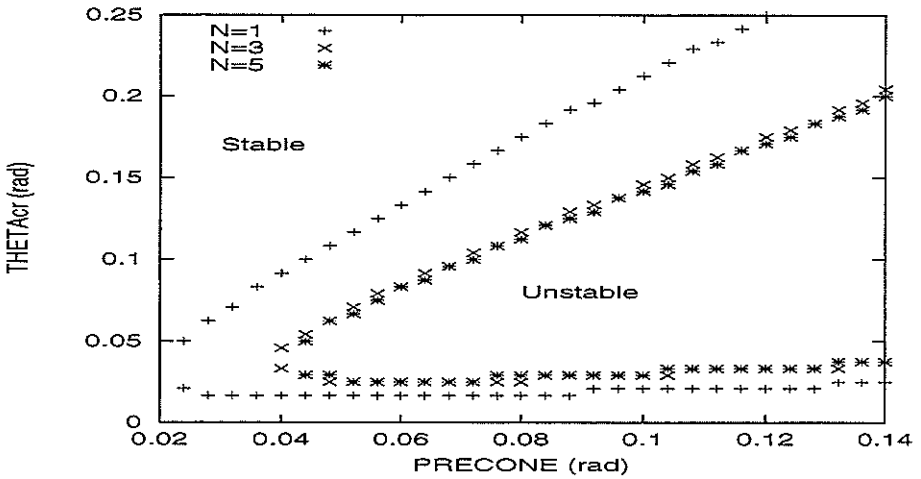

Figure 2: Stability boundary due to precone angle for stiff in-plane blade. Uniform-beam modes.

5. NUMERICAL RESULTS

In our numerical investigation, we have studied both the aeroelastic stability behavior of the hingeless blade considered, and its response to an external exitation caused by a vertical pulsating free-stream velocity.

For the stability analysis, we have determined the stability boundaries of a soft inplane blade and those of a stiff inplane blade, in terms of critical collective pitch angle *vs* the precone angle. In both cases, we have studied the convergence behavior of the solutions obtained using the three sets of mode shapes described in Section 3. The two blades considered have the fundamental flap natural frequency $\omega_w = 1.15\Omega$, with Ω denoting the angular velocity of the rotor. Furthermore, the soft inplane blade has the fundamental torsion natural frequency $\omega_\varphi = 2.5\Omega$, and the fundamental lead-lag natural frequency $\omega_v = 0.7\Omega$, whereas the stiff inplane blade has the fundamental torsion natural frequency $\omega_\varphi = 5\Omega$, and the fundamental lead-lag natural frequency $\omega_v = 1.5\Omega$.

Figure 1 depicts the stability boundaries of the soft inplane blade determined by the modal approach, with a different number of eigenfunctions of the nonrotating uniform beam. In this case, using 5 modes (per elastic displacement) seems to give a solution in terms of stability boundary that is very close to the converged one (*i.e.*, additional mode shapes do not alter significantly the

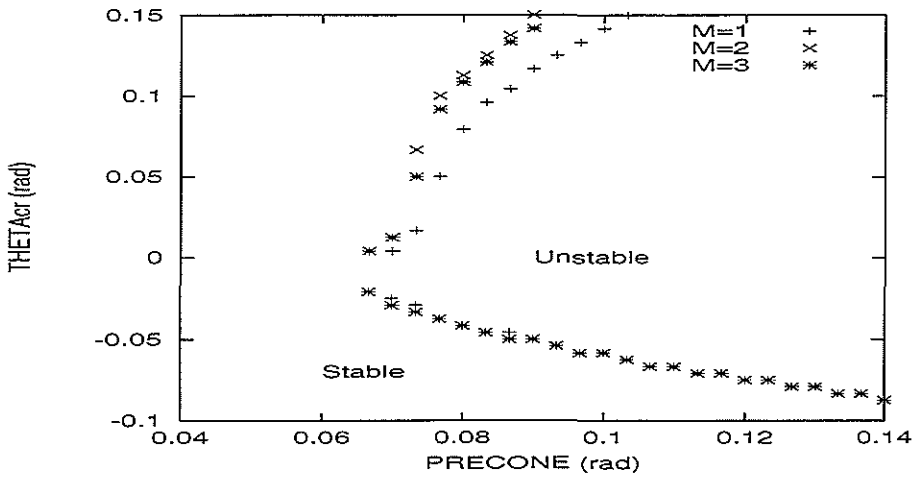

Figure 3: Stability boundary due to precone angle for soft in-plane blade. Equilibrium-independent rotating beam modes.

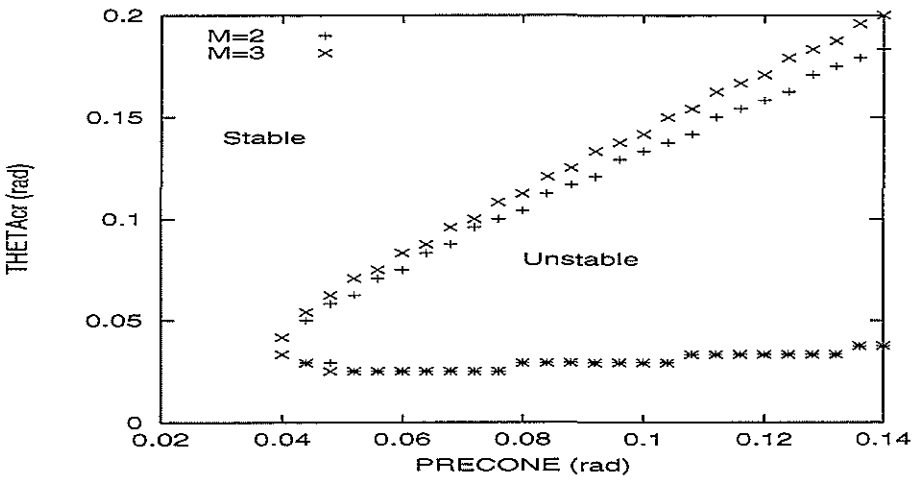

Figure 4: Stability boundary due to precone angle for stiff in-plane blade. Equilibrium-independent rotating beam modes.

stability boundary). A similar behavior of the solution is observed in Figure 2, where the stability boundaries are depicted for the stiff inplane blade, for elastic displacements expressed in terms of the eigenfunctions of the nonrotating uniform beam.

Then, Figure 3 and 4 illustrate, respectively, the stability boundaries of the soft and stiff in-plane blades, both obtained by the modal approach with mode shapes given by the eigenfunctions of the uncoupled-displacement rotating beam (*i.e.*, those independent on the steady equilibrium configuration). In this case, the convergence stability boundary appears to be determined using only 3 modes per elastic displacement.

Next, we have applied the modal approach by using the eigenfunctions of the coupled-displacement rotating beam, which depend on the steady equilibrium configuration. Figures 5 and 6 depict the soft inplane blade and the stiff inplane blade stability boundaries, respectively. In this case, the use of only one or two mode shapes seems to give a satisfactorily accurate prediction of the stability boundary.

Finally, we have studied the response of the blade to a vertical pulsating free-stream. Specifically, including in equations (7) and (13) the external aerodynamic forcing term due to the vertical

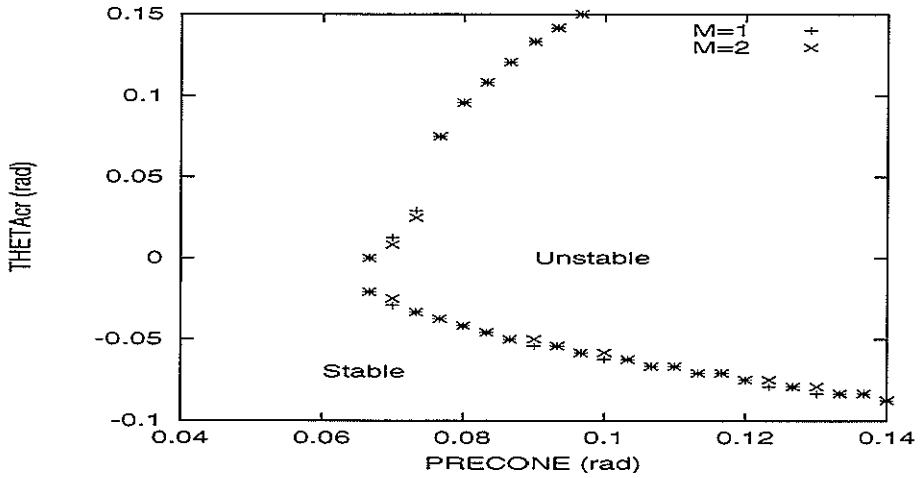

Figure 5: Stability boundary due to precone angle for soft in-plane blade. Equilibrium-dependent rotating beam modes.

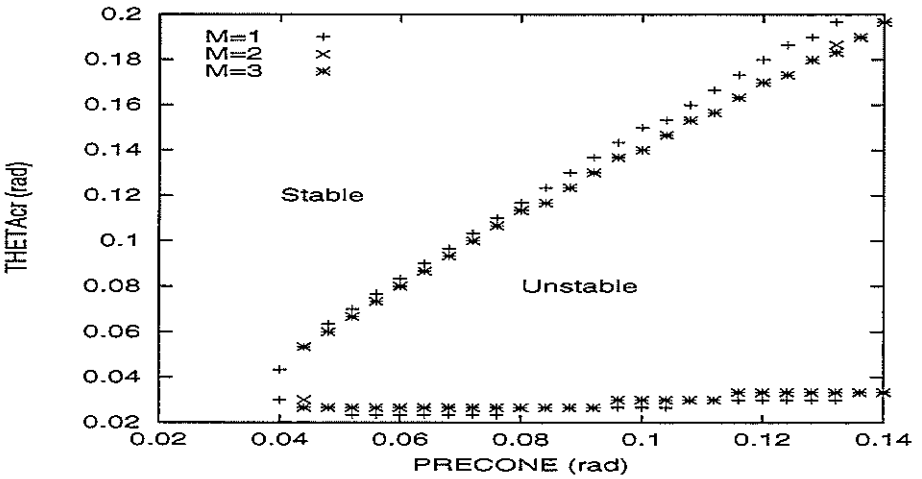

Figure 6: Stability boundary due to precone angle for stiff in-plane blade. Equilibrium-dependent rotating beam modes.

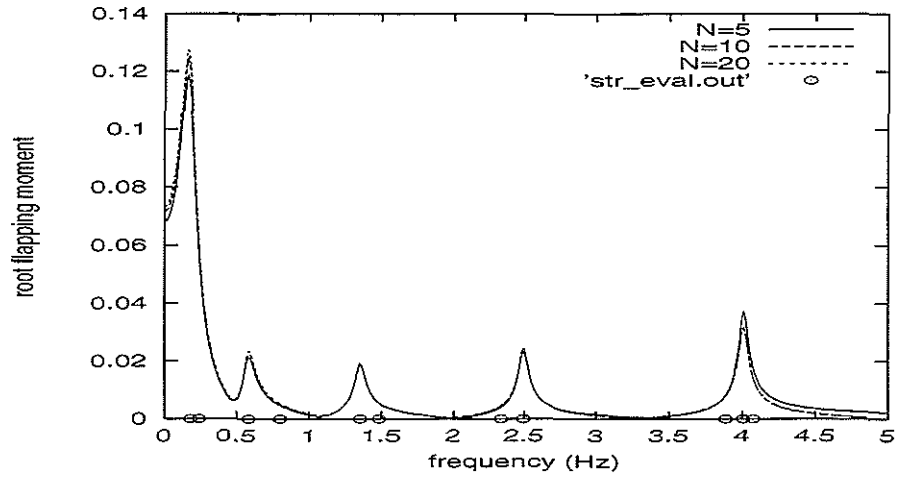

Figure 7: Amplitude of root-flapping-moment frequency response to a vertical pulsating free-stream. Modal approach using non-rotating uniform-blade modes.

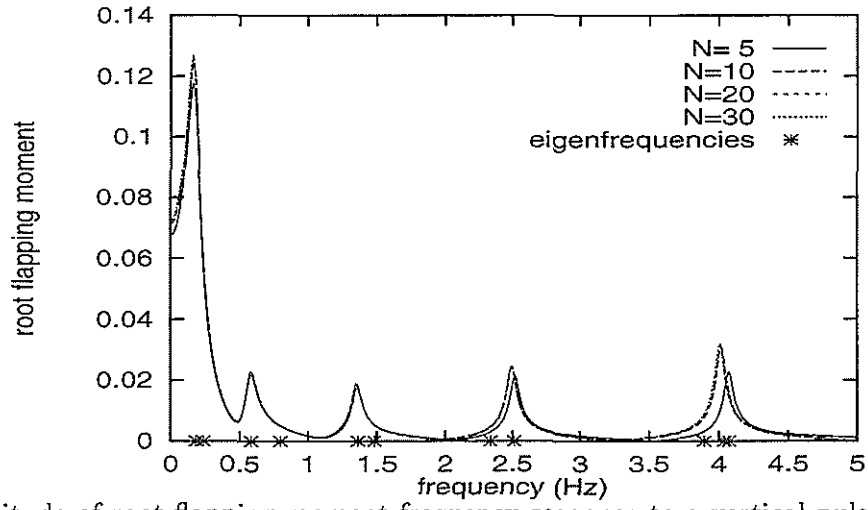

Figure 8: Amplitude of root-flapping-moment frequency response to a vertical pulsating free-stream. FEM approach.

free stream stemming from the quasi-steady aerodynamic theory considered, we have evaluated the spectrum of the unsteady elastic bending moment arising at the root of the cantilever blade with the collective pitch angle set equal to zero. The blade studied is the stiff inplane one, with $\omega_w = 1.15\Omega$ and $\omega_\varphi = 5\Omega$. In Figure 7 we depict the amplitude of the frequency responses obtained from the modal approach using different numbers of free-vibration modes of the nonrotating beam. In this case, the convergence of the response-peak values seems to be achieved with 20 modes, *i.e.*, with a very higher number of modes with respect to that needed for the stability-boundary convergence. The response analysis has been performed also using the FEM approach outlined in Section 4. The corrisponding results for different numbers of discretization elements on the blade, are illustrated in Figure 8 where the converged response appears to be achieved by the solution using 20 elements, although the 10-element solution gives a very accurate prediction of the root bending moment. From the comparison between Figures 7 and 8, one may observe that the two convergence histories reveal a similar behavior in terms of rapidity, and this demostrate that the use of modal approach is not more convenient with respect to the FEM one when local stress analysis is performed.

5. CONCLUDING REMARKS

The aeroelastic stability and response analysis for a cantilever flap-lag-torsion motion blade has been performed.

Specifically, we have analyzed the convergence behavior of solutions obtained using different mode shape sets in a modal approach, and using a FEM approach. As expected, in the stability boundary analysis (where the relevant contribution is given by low-frequency modes) the modal approach has demontrated to be a very efficient tool having a fast convergence behavior. However, in the frequency response analysis performed in terms of the root flapping moment, the convergence histories from modal and FEM solutions appear to have very similar behaviors and the very fast convergence rate of modal approach-solution seems to be deteriorated.

REFERENCES

1. Hodges, D.H., and Ormiston, R.A., Stability of Elastic Bending and Torsion of Uniform Cantilever Rotor Blades in Hover with Variable Structural Coupling, NASA TN D-8192, 1976.

2. Kwon, O.J., Hodges, D.H., and Sankar, L.N., Stability of Hingeless Rotor in Hover Using Three-Dimensional Unsteady Aerodynamics, J. of the American Helicopter Society, 1991.

3. Karunamoorthy, S., and Peters, D.A., Use of Hierarchical Elastic Blade Equations and Automatic Trim for Rotor Response, Vertica, vol. 11, 1987.

4. Friedmann, P.P, and Straub., F., Application of the Finite Element Method to Rotary Wing Aeroelasticity, J. of the American Helicopter Society, vol. 25, n. 1, 1980.

5. Sivaneri, N.T., and Chopra, I., Dynamic Stability of a Rotor Blade Using Finite Element Analysis, AIAA J., vol. 20, n. 5, 1982.

6. Greenberg, J.M., Airfoil in Sinusoidal Motion in a Pulsating Stream, NACA TN-1326, 1947.

7. Hodges, D.H., and Dowell, E.H., Nonlinear Equation of Motion for the Elastic Bending and Torsion of Twisted Nonuniform Rotor Blades, NASA TN D-7818, 1974.

8. Houbolt, J.C., and Brooks, G.W., Differential Equations of Motion for Combined Flapwise Bending, Chordwise Bending, and Torsion of Twisted Nonuniform Rotor Blades, NACA R-1346, 1957.

9. Przemieniecki, J.S., Theory of Matrix Structural Analysis, McGraw-Hill, New York, 1968.

ACKNOWLEDGEMENTS

This work has been supported by Centro Italiano Ricerche Aerospaziali (C.I.R.A.), grant NR. 007/99: *"Sviluppo di modelli dinamici ed aerodinamici per l'aeroelasticità dei rotori a mozzo non fisso"*.

The authors wish to acknowledge Dr. R. Bacchi and Mr. A. Bassetti for their help in obtaining some of the numerical results presented.